



Characterization and technological properties of two clay soils in Republic of Congo

Moutou Joseph-Marie^{1,2*}, Loubaki Raunel¹, Nsongo Timothée³ and Foutou Paul Mozalin¹

¹Laboratory of Applied Mineral Chemistry (LACMA), Faculty of Science and Technology, Marien Ngouabi University, Congo

²Ecole Normale Supérieure, Marien Ngouabi University, Congo

³Research Group on Physicochemical and Mineralogical Properties of Materials, Faculty of Sci. and Tech., Marien Ngouabi University, Congo
jmsbmout@yahoo.fr

Available online at: www.isca.in, www.isca.me

Received 22nd September 2018, revised 7th January 2019, accepted 15th January 2019

Abstract

The determination of the physicochemical and mineralogical characteristics as well as the technological properties of two clays used by peasants in the making of fired clay bricks in the Madingou and Makonongo localities respectively in the Bouenza and Pool Departments of Congo-Brazzaville, is the general objective of this work. Particle size distribution and Atterberg limits were measured. X-rays diffraction supplemented by chemical analysis was used to determine the mineralogy of these soils. The water absorption, firing shrinkage and the flexural strength of the bricks made with these two types of soil and baked at different temperatures were measured. The MAD sample is of silty clay texture while the MAKO sample is sandy clay loam texture. These textures have made possible to manufacture fired clay products with these soils as clay. These soils are considered as moderately plastic inorganic clays. These materials have optimum molding properties and the estimated shrinkage is relatively small. X-ray diffraction and chemical analysis indicated that MAD is a kaolinitic clay containing small proportion of illite while MAKO is an illitico-kaolinitic clay with kaolinitic predominance. The iron oxide content associated with the presence of titanium oxide ensures a colored firing. The ternary diagrams taking into account the mineralogical composition and the chemical composition leads us to consider that these soils will give colored bodies. The water absorption obtained (15.53% for MAD and 14.43% for MAKO) indicates that the sherds obtained at 1150°C are porous and favorable for the production of structural ceramics (bricks, tiles, floor coverings, drainage pipes). Since MAD has not reached the optimal sintering temperature at 1150°C, it is possible to find other uses with MAD depending on the technological parameters corresponding to its optimal sintering temperature. With regard to the technological properties it is possible to manufacture ceramic tiles type red monoporosa, red birapida and majolica by making additions of materials containing limestone.

Keywords: Clay, mineral composition, physical properties, technological parameters.

Introduction

The clay raw materials possess a great interest in considering their uses in agriculture, civil engineering and environmental studies. Properties such as chemical inertness, geochemical purity, ease of access to clay deposits and low price are the cause¹. In the building, many pieces (bricks, roof tiles, floor and wall coverings) are made from clay raw materials. The majority of ceramic products are obtained by sintering, generally between 900 and 1500°C².

In Congo, the products of the ceramic industry, in particular tiles and sanitary ware are imported. The conditions for the development of a ceramics industry do not seem to come together due to a lack of knowledge of clay raw materials. In rural areas, buildings predominantly use raw clay (adobe brick) or fired clay brick. The locality of Madingou shows many buildings with fired clay bricks. An artisanal production of fired clay bricks is more or less locally produced. In the locality of Makonongo, there is also the presence of some production of fired clay bricks by local craftsmen in traditional furnaces.

Clay deposits consist of several minerals. These are presented with various dimensions. The study of the composition of the clay is therefore necessary³. Then it is important to learn in detail about the various production processes. This work aims at the characterization of clays extracted in the two localities, Madingou (MAD) and Makonongo (MAKO).

Methodology

Sampling sites localization: The samples were taken from two different departments in the south of the country (the BOUENZA department and the POOL department).

Madingou: The Figure-1 gives us the pedology of the Madingou area. Madingou according to the pedological map is located on a clay material from the middle schist-limestone. The geographical coordinates of MADINGOU are: Latitude: 4°9 '12 S Longitude: 13°33 '0 E. The sampling site is located about 2 km from the left bank of MASSANGA Lake located in the district "Capable" of Madingou.

The Figure-2 allows us to locate the locality of Makonongo in the Department of Pool. Makonongo is in the Pool and especially in Boko Prefecture.

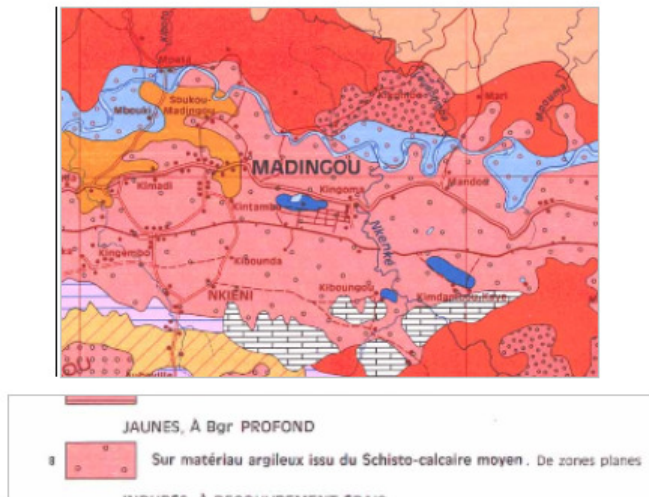


Figure-1: Pedological map of MADINGOU Area⁴.

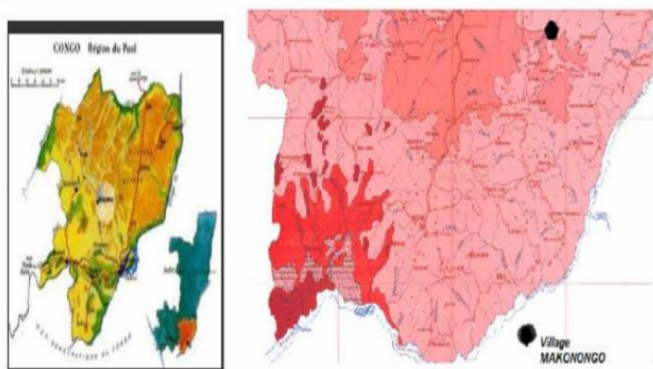


Figure-2: Location of Makonongo in the Pool Department⁴.

The soil of Makonongo is a clay-sandy material from Inkisi sandstone bordered with clay-silty and clay materials from schist-limestone.

Experimental methods: Physicochemical and mineralogical characterization: The limits of Atterberg were measured according to the standards NF P94-051⁵. The procedures described in the standards NF P 94-056⁵ and NF P 94-057⁵ made it possible to determine the proportions of the different particle classes. The X-ray pattern was recorded on a raw sample using a 'PANALYTICAL X'PERT PRO' 'K α 1 (0-20) diffractometer using Cu K α 1 radiation (45 kV, 40 mA) of the Institute of Condensed Matter Bordeaux Chemistry (ICMCB). The chemical composition in major elements was determined. In the Petrographic and Geological Research Center (CRPG) at Nancy (France).

Technological properties: Elaboration of the test specimens: A sample of clay soil is dried at 105°C in an oven. Grinding and 2mm sieving are applied. After weighing of a given mass and

humidification taking into account the results of the Proctor test, bricks are shaped with a mold of 4cmx4cmx16cm dimensions. The bricks are dried in the open air for 28 days and then fired at different temperatures in a muffle furnace.

Determination of the technological properties: The linear shrinkage is measured using sliding calipers. Let L_0 and L , the lengths of the bricks before and after the heat treatment the linear shrinkage is given by the following relation:

$$R_L = \left(\frac{(L_0 - L)}{L_0} \right) \times 100 \quad (1)$$

The 3-point flexion strength was measured according to EN 196-1 norm⁶. The water absorption water is carried out according to ASTM C 20-74⁷.

Results and discussion

The Figures-3(a and b) give us the particle size distribution curves of the MAD and MAK0 samples.

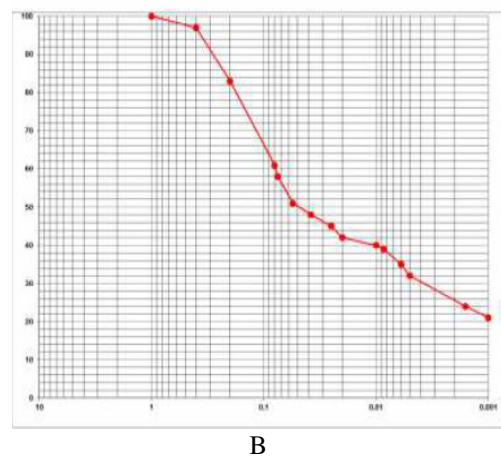
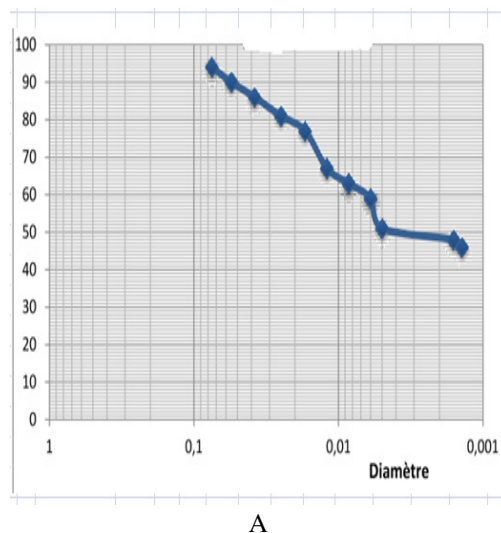


Figure-3: MAD (a) and MAKO (b) particle size distribution curves.

The observation of these two curves reveals that MAD has moderately tight particle size distribution while that of MAKO is spread. The particle size distributions of these clays are given in the Table-1.

Table-1: Particle size distribution.

Particle	MAKO	MAD
Clay	24	48
Silt	18	42
Sand	58	10

The positioning of these clays in texture triangle is given in the Figure-4.

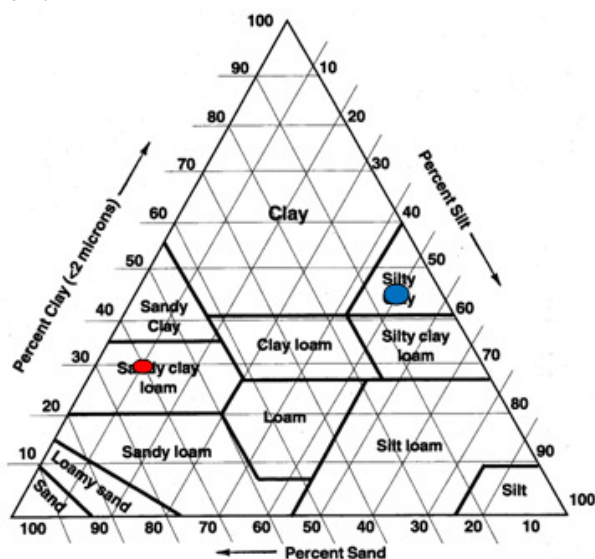


Figure-4: Positioning of MAKO and MAD in texture triangle⁸.

The positioning of the MAKO and MAD samples in the USDA textural triangle of Soil Survey Manual⁸ indicates that these two soils have respectively silty-clay-sandy and clay-silty textures. In order to clarify the use in structural (building) ceramics, we have positioned these soils in the Winkler diagram⁹ (Figure-5).

MAKO clay with a coarse grain size would be suitable for making vertical perforation bricks while MAD with a relatively finer grain size would be the raw material for roofing tiles. Dondi et al. examined the texture of clays (mixtures or clays alone) most frequently used in Italy for manufacturing of building ceramics⁹. The Shepard classification¹⁰ was used in this study. This latter considers the following fractions: >63 μm , 4-63 μm and <4 μm . Therefore the percentages of the different fractions are shown in the Table-2.

The Figure-6 shows the texture domains in the Shepard diagram of Italian clays taking into account their frequency of use in the ceramic industry.

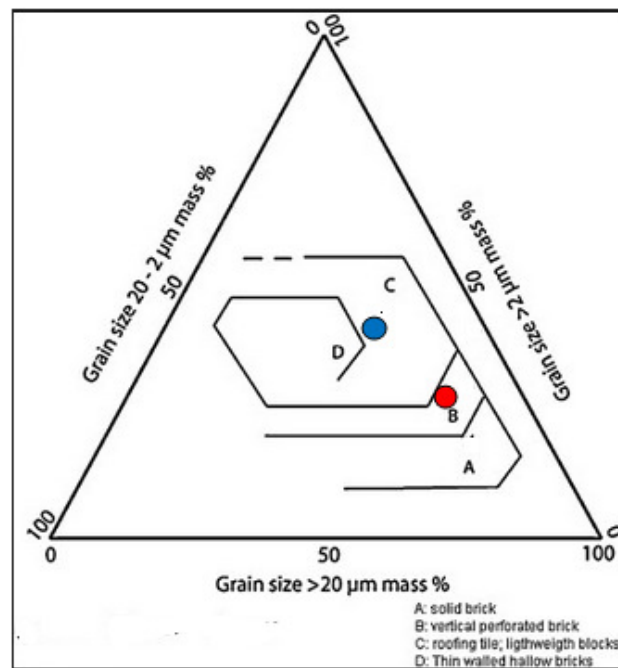


Figure-5: Positioning of MAKO and MAD in the Winkler diagram⁹.

Table-2: Particle size distribution applied in the Shepard diagram.

Particle	MAKO	MAD
Clay < 4	30%	49%
Silt 4 – 63	24%	41%
Sand > 63	46%	10%

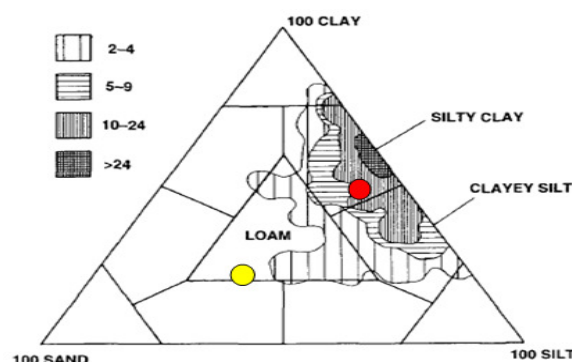


Figure-6: Positioning of MAD and MAKO in Shepard diagram⁹.

Considering the results from this study, the silty clays and clayey silt textures correspond to raw materials mainly used to clay products for building. According to the classification of Shepard, MAD is of silty clay type and located in a zone of frequency between 10 and 24 whereas MAKO is silty. The Table-3 gives us the Atterberg limits of the two samples.

Table-3: Atterberg limits.

Localities	Liquidity limit	Plasticity limit	Plasticity index
MAD	46,8	23,6	23,2
MAKO	38,8	16	22,8

Despite the difference in particle size distribution, in particular the large difference in fine fraction ($<2 \mu\text{m}$), the plasticity indices of these two clays are practically identical. The liquidity limits are very different ($\text{MAD} > \text{MAKO}$). The I_p values allow us to deduce that these soils are moderately plastic. The Figure-7 positions the MAD and MAKO samples in the Casagrande abacus¹¹ to assess their degree of plasticity.

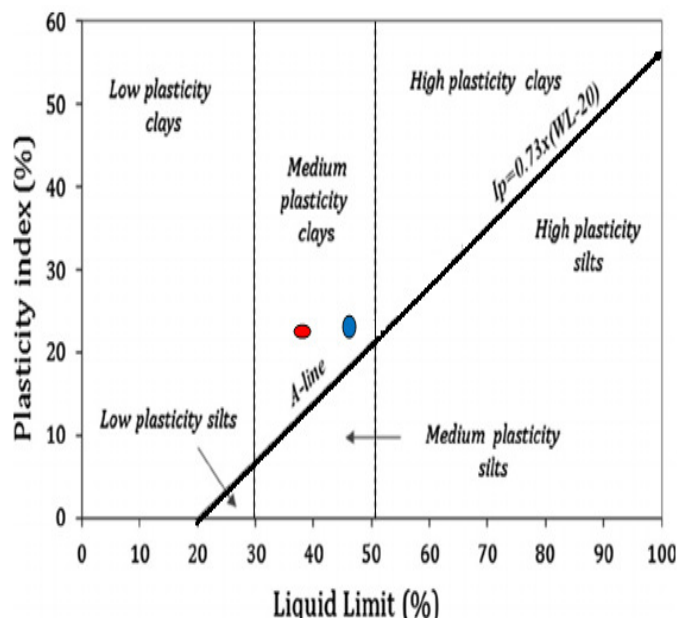


Figure-7: Positioning of MAD and MAKO in the Casagrande abacus¹¹.

The positioning in the Casagrande abacus indicates that MAKO and MAD are inorganic clays of medium plasticity. MAD is closer to the zone of high plasticity than MAKO. This observation can be related to the particle-size distribution of these two clays. MAD with a larger proportion of clay presents a larger liquidity limit. The Figure-8 allows us to appreciate the molding properties of the two clays.

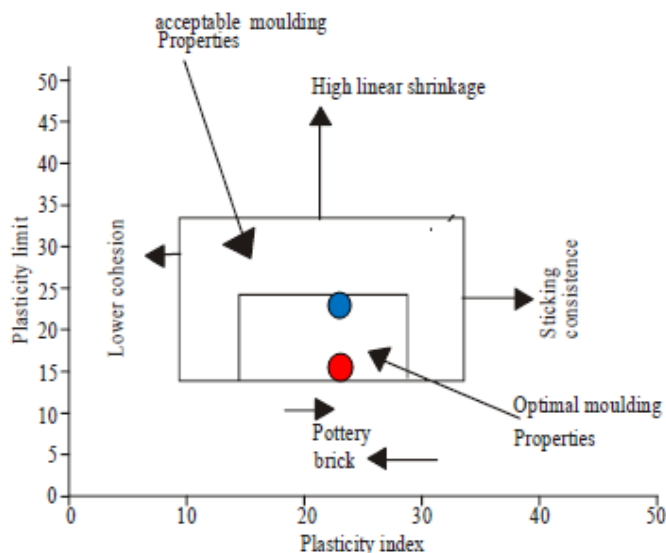


Figure-8: Positions of MAD and MAKO clays in workability chart¹¹.

Both MAKO and MAD samples are located in the field of optimal molding properties. But their disposition in this chart indicates that MAD would show a larger shrinkage than MAKO. This is in accord with the high clay content in MAD than in MAKO. Figure-9 represents X-rays patterns for MAD and MAKO.

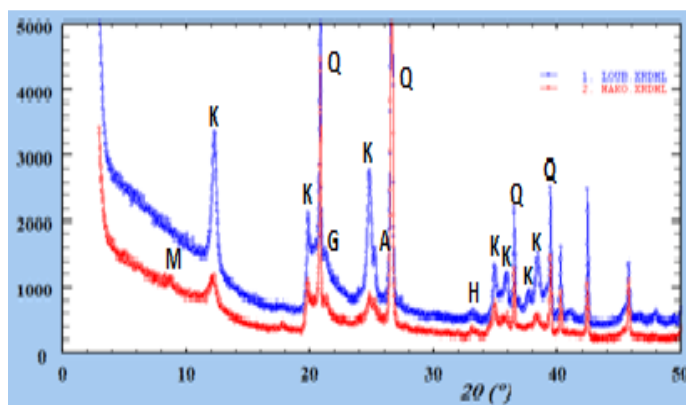


Figure-9: X-ray pattern of MAD (blue) and MAKO (red) clays.

The Table-4 gives us the chemical composition of MAD and MAKO.

Table-4: chemical composition of MAKO and MAD

Localities	SiO ₂	Al ₂ O ₃	Fe ₂ O ₃	MnO	MgO	CaO	Na ₂ O	K ₂ O	TiO ₂	P ₂ O ₅	PF	Total
MAD	59,92	22,72	3,94	<L.D.	0,10	0,04	0,02	0,33	1,56	0,12	11,06	99,80
MAKO	60,26	19,56	5,66	<L.D.	0,60	<L.D.	0,03	1,21	0,95	<L.D.	12,02	100,29

Analysis of the two spectra reveals the presence of kaolinite with the peaks at 7.21, 4.46, 3.58, 2.56, 2.53 and 2.50Å.^{12,13} Quartz is indicated by well resolved peaks at 4.26 and 3.34Å. The comparison of the heights of the main peaks of kaolinite in the two spectra gives a MAD/MAKO ratio equal to approximately 3. This ratio is in harmony with the results of the particle size analysis. In the interval between 20° (2θ) - 22° (2θ), the (02l) and (11l) reflections are not distinct. So we deduce that in MAD and MAKO, kaolinite is disordered¹⁴. The distinct observation of peaks of relatively low intensity at 8.75° and 17.82° (2θ) corresponding respectively to spacings of 10.14Å and 4.97Å in MAKO supposes the presence of illite. The K₂O content, higher in MAKO than in MAD, leads to consider a more significant content of illite in MAKO than in MAD. The higher illite content in MAKO could explain the almost identical value of the plasticity index of two samples despite a difference in the proportion of their clay fraction. In fact illite has greater plasticity than kaolinite¹⁵. The MgO percentage in MAD (0.10%) and MAKO (0.60%) would suggest the presence of carbonate of very low abundance. The peak at 4.18Å is attributed to goethite¹².

The presence of hematite is reported in both spectra, from the peak at 2.7Å. The peak of hematite is of higher intensity in MAKO than MAD. This confirms the relatively high levels of iron oxides in MAD (5,66%) and in MAKO (3,94%). Anatase and rutile (titanium oxides) are reported respectively by the peak at 3.4Å (25.264° 2θ) and the peak at 3.2Å (27.39° 2θ). The peak at 3.2Å could also indicate the microcline. The SiO₂ / Al₂O₃ ratios in MAD (2,637) and MAKO (3,081) reveal a higher amount of quartz in MAKO than in MAD.

The presence of TiO₂ (1.56 for MAD and 0.95 for MAKO) associated with significant Fe₂O₃ contents indicates a colored firing with these two samples. The Figure-10 gives us the positioning of the MAKO and MAD samples in the ternary diagram according to the chemical composition¹⁶.

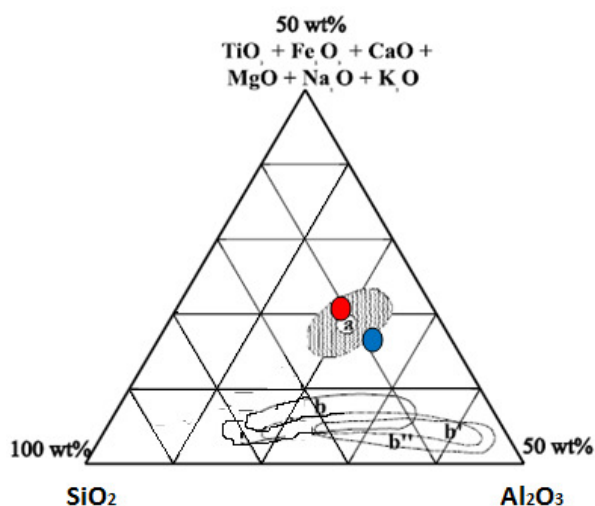


Figure-10: Fabbri and Fiori diagram (chemical composition)¹⁶.

The zones marked b, b' and b'' correspond to white bodies. The area marked "a", indicates red stonewares. MAKO and MAD are both near the red stonewares area.

The Table-5 gives us the estimated mineralogical balance¹¹.

MAD could be classified as kaolinitic clay while MAKO should be an illitico-kaolinitic clay¹¹ dominated by kaolinite. The content of clay minerals is greater in MAD (57,6%) than in MAKO (49,83%). This is in agreement with the results of the particle size distribution. The sum of the mineral contents being less than 100% in MAKO suggests that the quartz content is underestimated with regard to the particle size distribution. The mineralogical balance seems to agree with the calculation of activity according to Skempton¹⁷. The activity calculated using the Skempton formula is 0.47 for the MAD sample confirming a predominance of kaolinite, while it is equal to 0.95 for the MAKO sample thus corresponding to the relative abundance of more active clay (illite).

The abundance of illite and iron oxides in MAKO would suggest the presence of liquid phase during sintering in MAKO. In fact, illite and iron oxides generally act as fluxes¹⁸. The loss on ignition in MAKO is greater than that of MAD. This could be explained by the presence of goethite in greater quantity in MAKO. These MAD and MAKO clays can be used for the production of large-scale ceramics such as tiles, tiles or bricks. The Figure-11 illustrates the ternary diagram established on the mineralogical composition.

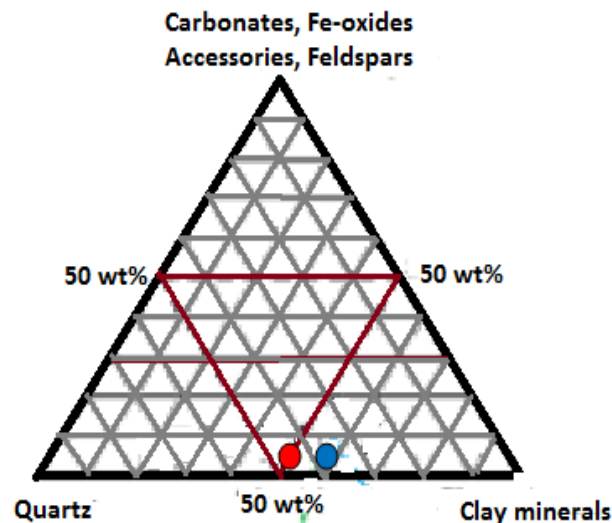


Figure-11: Ternary diagram (mineralogical composition)¹⁹.

The positioning of MAD and MAKO in the ternary diagram of Fiori et al.¹⁹ (Figure-11) would indicate that MAKO would be favorable than MAD for manufacturing porous ceramic bodies. The positioning of MAD in Augustinik diagram²⁰ (Figure-12) is close to the area suitable for making sandstone while MAKO is a sandstone and can be used to manufacture hollow products. The Figures-13 and 14 present the evolution of technological properties of MAD and MAKO clays.

Table-5: Mineralogical balance.

Localities	Illite	Kaolinite	Quartz	Hématite	Rutile	Sum
MAD	2,79	54,81	37,2	3,94	1,56	100,3%
MAKO	10,25	39,58	37,6	5,66	0,95	94,04%

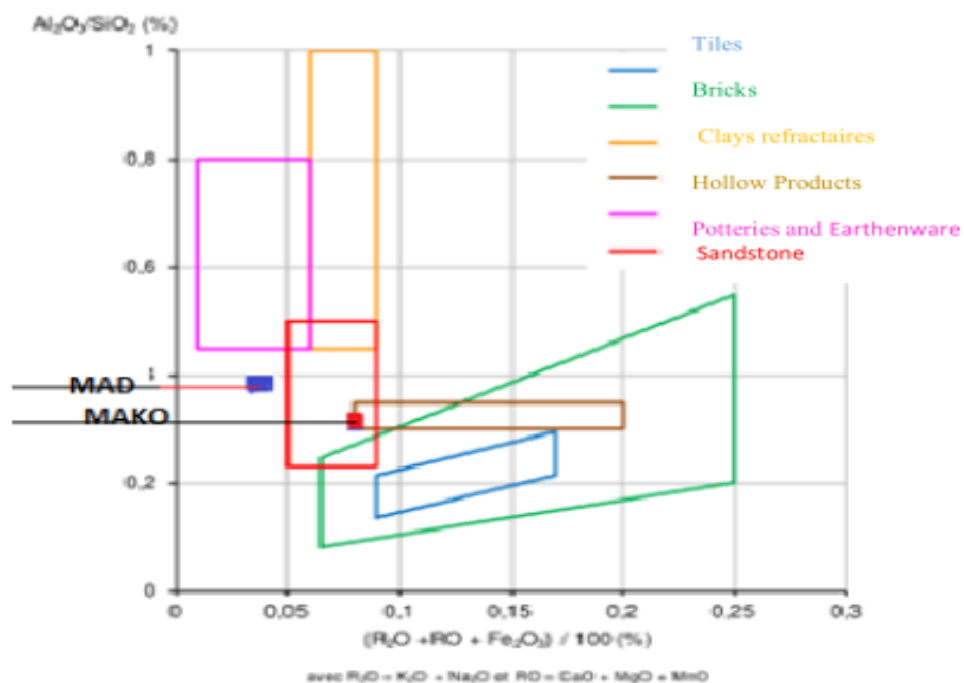


Figure-12: Positioning of MAD and MAKO clays in Augustinik diagram²⁰.

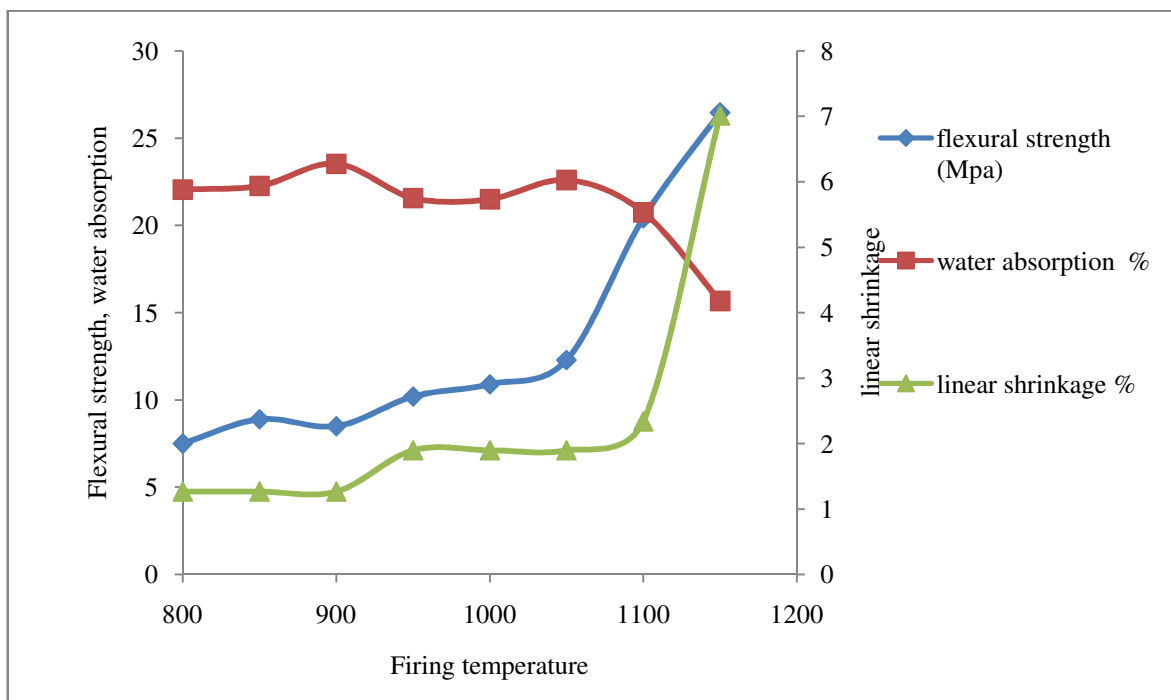


Figure-13: Technological properties of MAD.

The flexural strength and the linear shrinkage of the two clays show the same tendencies, i.e. they show a low growth between 800°C and 1050°C and increase sharply from 1050°C. While the water absorption has an inverse tendency, its evolution corresponds practically to a plateau between 800°C and 1050°C and decreases sharply from 1050°C.

MAD and MAKO materials with water absorption values $\leq 20\%$ could be used in the manufacture of roofing tiles but unsuitable for the manufacture of floor tiles²¹. The water absorption of MAKO (14.49%) and MAD (15.67%) correspond to the requirements of the Spanish association of ceramics and tiles for covering ceramic tiles²².

The values obtained for MAKO (32.08MPa) and for MAD (26.45MPa) satisfy the requirements of the standards for fabrication of paving and roofing tiles²². The values reached at 1150°C for the linear shrinkage show that shrinkage is greater in MAD (7.01%) than in MAKO (5.15%). Indeed MAD possess a highest fine fraction ($<2\mu\text{m}$) than MAKO. It has been shown that linear low firing shrinkages are achieved with significant quartz levels in clay raw materials²³. Firing linear shrinkage ($<10\%$) allows MAD and MAKO clays to be used in the manufacture of ceramics. The Figures-15, 16 and 17 compare the evolution of water absorption, linear shrinkage and flexural strength with the firing temperature in the MAD and MAKO samples.

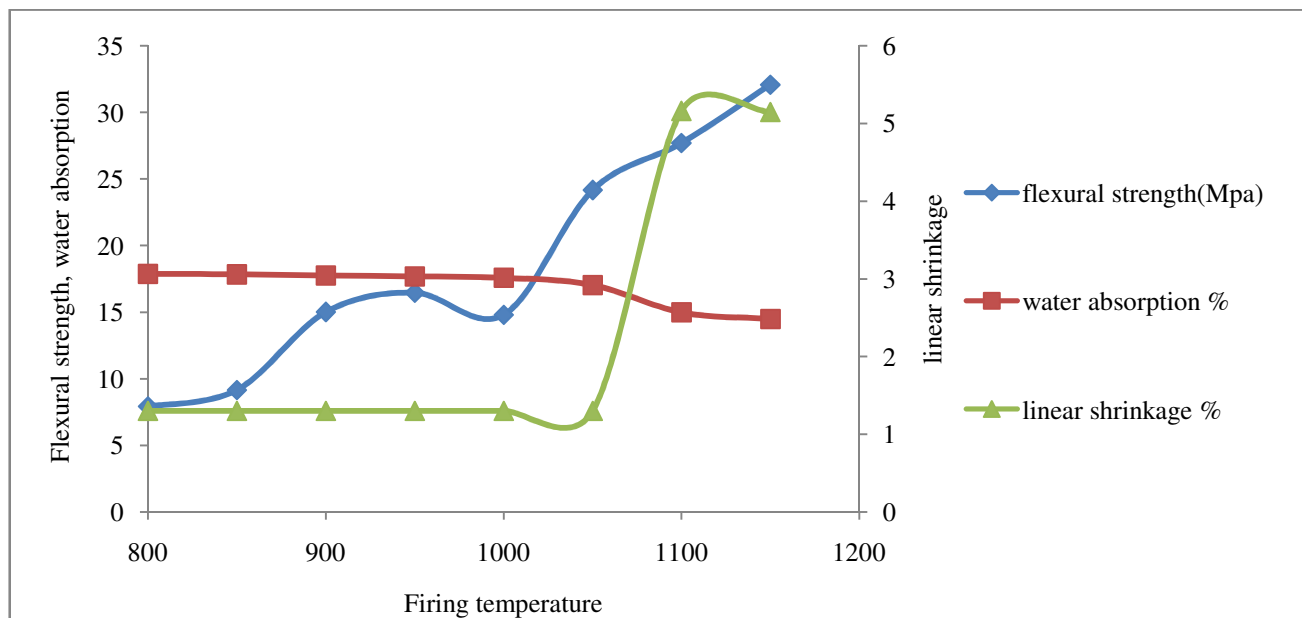


Figure-14: Technological properties of MAKO.

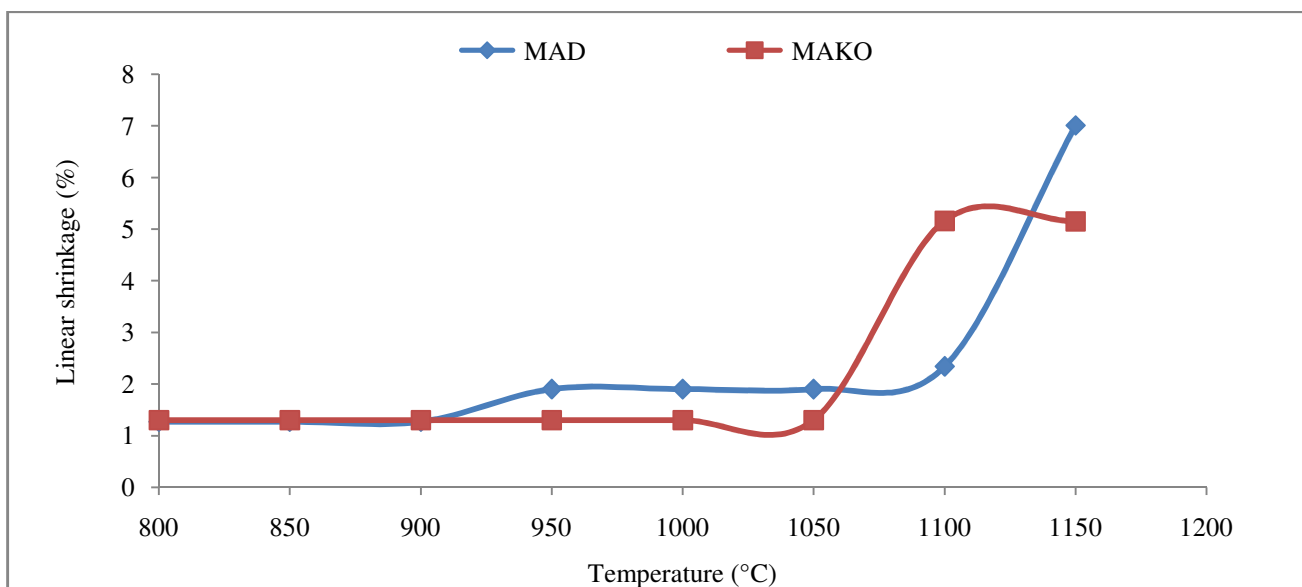


Figure-15: Evolution of linear shrinkage in MAD and MAKO.

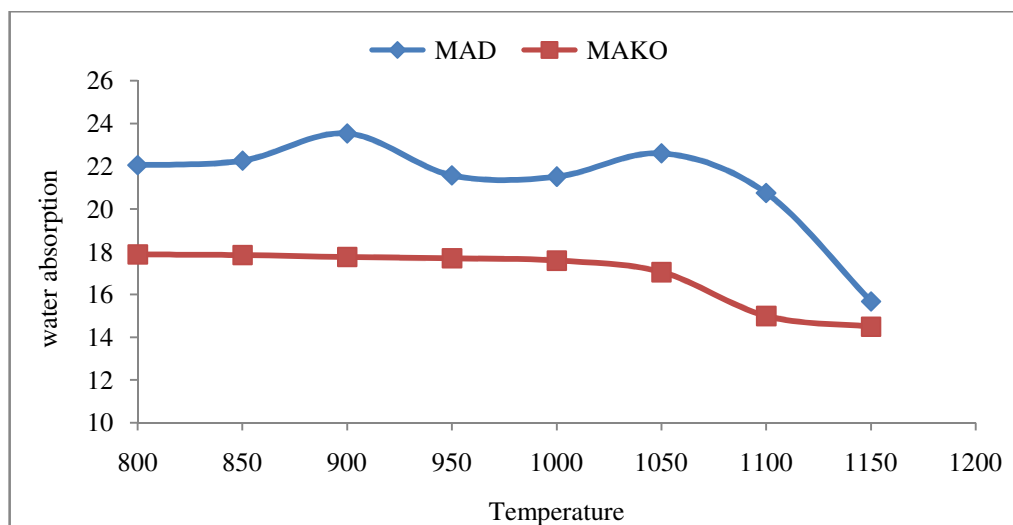


Figure-16: Evolution of water absorption in MAD and MAKO.

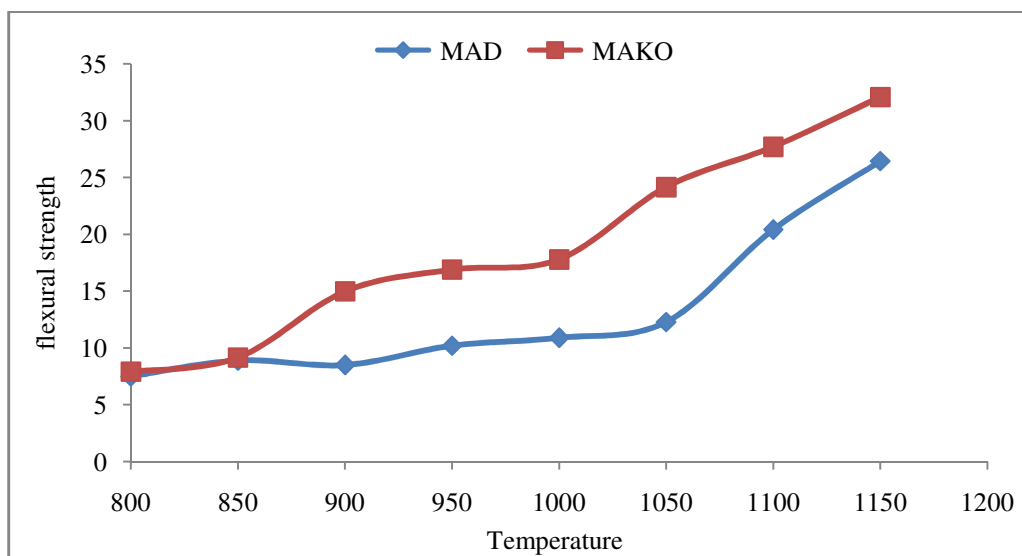


Figure-17: Evolution of flexural strength in MAD and MAKO.

Linear shrinkage between 950°C and 1050°C is greater in MAD than in MAKO. This phenomenon is attributed to the structural reorganization of metakaolinite²⁴. The higher kaolinite content in MAD (54.81% by weight against 39.58% in MAKO) justifies this observation. Thus we can interpret the rapid evolution of the linear shrinkage at 1100°C of MAKO by its illite content (10.25%) much higher than that of MAD (2.79%). The densification in MAD starts only from 1150°C. The smaller shrinkage in MAKO at 1150°C compared to MAD would be explained by a more abundant presence of quartz that has not been dissolved in the flux. The abundance of quartz favors a more open microstructure that prevents densification²⁴.

The heat treatment at these temperatures causes the departure of water molecules and other volatile substances such as CO₂ from the combustion of organic matter and the decomposition of carbonates, the SO₃ from sulphate decomposition, P₂O₅ and air

trapped during mixing. The expulsion of volatile substances favors the production of open porosity. However, the percentage of water in kaolinite is greater than that of illite. Consequently, the quantity of water released by MAD is therefore greater than that of MAKO. We can thus explain that the absorption water of MAD is much higher than that of MAKO up to 1050°C. From 1050°C, the liquid phase resulting from illites by bringing the solid particles together considerably reduces the open porosity therefore the water absorption. Unlike MAKO, MAD has a relatively weak quartz content that does not effectively resist densification. If MAKO shows a low variation of the absorption water starting from 1050°C (from 17.04 to 14.49), the variation at the level of MAD is greater (from 22.6 to 15.67). The fact that the evolution of the absorption water and the linear shrinkage of MAKO tend to achieve a plateau from 1100°C leads us to consider that MAKO at 1100°C has reached its maximum densification.

On the other hand the evolution of the absorption water and the linear shrinkage of MAD not having reached a plateau, leads us to think that MAD did not reach its densification maximum. Since the linear shrinkage of MAD is greater than that of MAKO from 950°C to 1050°C, it is expected that the mechanical strength of MAD is higher than that of MAKO. We observe rather the opposite. Indeed, high kaolinite content prevents clays from reaching high mechanical strength, despite their high densification. We believe that the relatively large linear shrinkage in MAD in the 950°C-1050°C temperature range causes structural microcracks consistent with the higher absorption water in MAD. These structural microcracks reduce the mechanical strength of the fired materials. Thus we can explain why the mechanical flexural strength of MAKO is greater than that of MAD in this interval. The liquid phase formation above 1000°C reduces porosity, which hinders crack formation and improves the mechanical strength. From 1050°C, the slope of the evolution of the mechanical strength of MAD is almost twice that of MAKO. MAD and MAKO agree to the realization of fired clay products.

Conclusion

To determine the physicochemical and mineralogical characteristics and the technological properties of two clays used by farmers in the manufacture of clay bricks in the localities of Madingou (Bouenza department) and Makonongo (Pool department) in Congo-Brazzaville is the overall objective of this study.

The MAD sample is of silty clay texture while the MAKO sample is sandy clay loam texture. The particle size distribution has made it possible to classify as clay raw material for the manufacture of fired clay products. These soils consist of moderately plastic inorganic clays. These materials have optimum molding properties and the estimated shrinkage is relatively small. X-ray diffraction and chemical analysis indicated that MAD is a kaolinitic clay containing a little illite while MAKO is a illitico-kaolinitic clay with kaolinitic predominance. The iron oxide content associated with the presence of titanium oxide ensures a colored firing. The ternary diagrams taking into account the mineralogical composition and the chemical composition made it possible to consider that these soils were adapted for the realization. The absorption water obtained (15.53% for MAD and 14.43% for MAKO) made it possible to deduce that the bodies fired at 1150°C are porous favorable for the production of structural ceramics (bricks, tiles, floor coverings, drainage pipes). Since MAD has not reached the optimum sintering temperature at 1150°C, it is possible to find other uses with MAD depending on the technological parameters corresponding to its optimal sintering temperature.

References

1. Konta J. (1995). Clay and man: Clay raw materials in the service of man. *Applied Clay Science*, 10(4), 275-335.

2. Wetshondo Osomba D. (2012). Caractérisation et valorisation des matériaux argileux de la Province de Kinshasa (RD Congo). Thèse de docteur ingénieur, Université de Liège (Belgique), 1-341.
3. Freyburg S. and Schwarz A. (2007). Influence of the clay type on the pore structure of structural ceramics. *ECERS*, 27(2-3), 1727-1733.
4. Denis B. and Rieffel J. (1975). Notice explicative N° 60; Carte Pédologique du Congo à 1/200,000. *feuille Madingou; ORSTOM: Office de la Recherche Scientifique et Technique Outre-Mer; Paris*, 1-152.
5. Moutou J.M., Bibila Mafoumba C., Matini L., Ngoro Elenga F. and Kouhounina L. (2018). Characterization and evaluation of the adsorption capacity of dichromate ions by a clay soil of Impfondo. *Research Journal of Chemical Sciences*, 8(4), 1-14.
6. NF EN 196-1 (2006). Méthodes d'essais des ciments – Partie 1 : déterminations des résistances mécaniques. *Norme française*, AFNOR.
7. ASTM C 20-00 (2010). Standard Test Methods for Apparent Porosity, Water Absorption, Apparent Specific Gravity, and Bulk Density of Burned Refractory Brick and Shapes by Boiling Water I.
8. Soil Science Division Staff (2017). Soil survey manual. Ditzler C., Scheffe K. and Monger H.C., USDA Handbook 18. Government Printing Office Washington D.C., 1-639.
9. Dondi M., Fabbri B. and Guarini G. (1998). Grain-size distribution of Italian raw materials for building clay products: a reappraisal of the Winkler diagram. *Clay Minerals*, 33(3), 435-442. <https://doi.org/10.1180/000985598545732>
10. Shepard F.P. (1954). Nomenclature based on sand-silt-clay ratios. *Journal of Sedimentary Petrology*, 24(3), 151-158.
11. Moutou J.M., Foutou P.M., Matini L., Banzouzi Samba V., Diamouangana Mpissi Z.F. and Loubaki R. (2018). Characterization and Evaluation of the Potential Uses of Mouyondzi Clay. *Journal of Minerals and Materials Characterization and Engineering*, 6, 119-138.
12. Brown G. and Brindley G.W. (1980). Crystal structures of clay minerals and their X-ray identification. London: Mineralogical Society, 5, 305-360.
13. Decarreau A. (1990). Matériaux argileux : Structure, propriétés et applications. Société française de Minéralogie et de Cristallographie et Groupe Français des Argiles, 1-586.
14. Plançon A., Giese R.F. and Snyder R. (1988). The Hinckley index for kaolinites. *Clay Minerals*, 23(3), 249-260.
15. Mitchell James K. and Kenichi S. (1993). Fundamentals of soil behavior. Third Edition John Wiley & Sons, 1-560.

16. Fabbri B. and Fiori C. (1985). Clays and complementary raw materials for stoneware tiles. *Miner. Petrogr. Acta*, 29-A, 535-545.
17. Skempton A.W. (1953). The colloidal “activity” of clays. *Proceedings of the 3rd International Conference of Soil Mechanics and Foundation Engineering*, 1, 57-60.
18. Hosterman J.W. (1969). Clay deposits of Spokane County Washington. *Geological Survey Bulletin* 1270, 1-96. <https://doi.org/10.3133/b1270>
19. Fiori C., Fabbri B., Donati G. and Venturi I. (1989). Mineralogical composition of the clay bodies used in the Italian Tile Industry. *Applied Clay Science*, 4(5-6), 461-473.
20. Haurine F. (2015). Caractérisation d'atterrissements d'argiles récents sur le territoire français, en vue de leur valorisation dans l'industrie des matériaux de construction en terre cuite. *Sciences de la Terre*, Thèse de Doctorat, École nationale supérieure des mines de Paris, 1-327.
21. Souza G.P., Sanchez R. and de Holanda J.N.F. (2002). Characteristics and physical-mechanical properties of fired kaolinitic materials. *Cerâmica*, 48(306), 102-107.
22. Romero M., Andrés A., Alonso R., Viguri J. and Rincon J. Ma. (2008). Sintering behaviour of ceramic bodies from contaminated marine sediments. *Ceramics International*, 34(8), 1917-1924.
23. Correia S.L., Hotza D., Segadães A.M. (2004). Effect of Raw Materials on Linear Shrinkage. *Am. Ceram. Soc. Bulletin*, 83(8), 9101-9108.
24. Calata J.N. (2005). Densification behavior of ceramic and crystallizable glass materials constrained on a rigid substrate. Ph.D. Thesis Virginia Polytechnic Institute, 1-167.